International Journal of Control
Publication details, including instructions for authors and subscription information:
http://www.informaworld.com/smpp/title~content=t713393989

A two-tier control architecture for nonlinear process systems with continuous/asynchronous feedback

Jinfeng Liu [a]; David Muñoz de la Peña [b]; Benjamin J. Ohran [a]; Panagiotis D. Christofides [ac]; James F. Davis [a]
[a] Department of Chemical and Biomolecular Engineering, University of California, Los Angeles, CA 90095-1592, USA [b] Departamento de Ingeniería de Sistemas y Automática, Universidad de Sevilla, Sevilla, Spain [c] Department of Electrical Engineering, University of California, Los Angeles, CA 90095-1592, USA

First published on: 13 October 2009

To cite this Article Liu, Jinfeng, Muñoz de la Peña, David, Ohran, Benjamin J., Christofides, Panagiotis D. and Davis, James F.(2010) 'A two-tier control architecture for nonlinear process systems with continuous/asynchronous feedback', International Journal of Control, 83: 2, 257 — 272, First published on: 13 October 2009 (iFirst)
To link to this Article: DOI: 10.1080/00207170903141051
URL: http://dx.doi.org/10.1080/00207170903141051

International Journal of Control
Vol. 83, No. 2, February 2010, 257–272

Taylor & Francis
Taylor & Francis Group

A two-tier control architecture for nonlinear process systems with continuous/asynchronous feedback

Jinfeng Liu[a], David Muñoz de la Peña[b], Benjamin J. Ohran[a], Panagiotis D. Christofides[ac]* and James F. Davis[a]

[a]*Department of Chemical and Biomolecular Engineering, University of California, Los Angeles, CA 90095-1592, USA;* [b]*Departamento de Ingeniería de Sistemas y Automática, Universidad de Sevilla, Camino de los Descubrimientos S/N, 41092, Sevilla, Spain;* [c]*Department of Electrical Engineering, University of California, Los Angeles, CA 90095-1592, USA*

(*Received 18 June 2008; final version received 23 June 2009*)

In this work, we introduce a two-tier control architecture for nonlinear process systems with both continuous and asynchronous sensing and actuation. This class of systems arises naturally in the context of process control systems based on hybrid communication networks (i.e. point-to-point wired links integrated with networked wired or wireless communication) and utilising multiple heterogeneous measurements (e.g. temperature and concentration). Assuming that there exists a lower-tier control system which relies on point-to-point communication and continuous measurements to stabilise the closed-loop system, we propose to use Lyapunov-based model predictive control to design an upper-tier networked control system to profit from both the continuous and the asynchronous measurements as well as from additional networked control actuators. The proposed two-tier control system architecture preserves the stability properties of the lower-tier controller while improving the closed-loop performance. The theoretical results are demonstrated using two different chemical process examples.

Keywords: networked control systems; model predictive control; nonlinear systems; fault-tolerant control systems; process control applications

1. Introduction

Increasingly faced with the requirements of safety, environmental sustainability and profitability, chemical process operation is relying extensively on highly automated control systems. Traditionally, control systems utilise point-to-point wired communication links using a small number of sensors and actuators. The operation of chemical processes, therefore, could benefit from the deployment of control systems using hybrid communication networks that take advantage of an efficient integration of the existing, point-to-point communication networks (wire connections from each actuator or sensor to the control system using dedicated local area networks) and additional networked (wired or wireless) actuator and sensor devices. Such an augmentation in sensor information and network-based availability of wired and wireless data is now well under way in the process industries (Ydstie 2002; Davis 2007; Neumann 2007; Christofides et al. 2007) and clearly has the potential to be transformative in the sense of dramatically improving the ability of the single-process and plantwide model-based control systems to optimise process and plant performance (in terms of achieving control objectives that go well beyond the ones that can be achieved with control systems using wired, point-to-point connections) and prevent or deal with adverse and emergency situations more quickly and effectively (fault-tolerance). Hybrid communication networks allow for easy modification of the control strategy by rerouting signals, having redundant systems that can be activated automatically when component failure occurs, and, in general, they allow having a high-level supervisory control over the entire process (Ydstie 2002; Davis 2007; Neumann 2007; Christofides et al. 2007). However, augmenting existing control networks with real-time wired or wireless sensor and actuator networks challenges many of the assumptions in traditional process control methods dealing with dynamical systems linked through ideal channels with flawless, continuous communication. In the context of hybrid communication networks which utilise networked sensors and actuators, key issues that are important for process control include robustness, reliability and interference. These issues need to be carefully handled because integrated wired and wireless communication networks

*Corresponding author. Email: pdc@seas.ucla.edu

ISSN 0020–7179 print/ISSN 1366–5820 online

DOI: 10.1080/00207170903141051
http://www.informaworld.com

introduce more components in order to substantially improve closed-loop performance and fault-tolerance, and this increases the probability of missing data at any given point in time.

Within control theory, the study of control over networks has attracted considerable attention in the literature (Nair and Evans 2000; Brockett and Liberzon 2000; Christofides and El-Farra 2005; Mhaskar, Gani, McFall, Christofides, and Davis 2007) and early research focused on analysing and scheduling real-time network traffic (Shin 1991; Hong 1995). Research has also studied the stability of network-based control systems. A common approach is to insert network behaviour between the nodes of a conventional control loop. In Walsh, Ye, and Bushnell (2002) it was proposed to first design the controller using established techniques considering the network transparent, and then to analyse the effect of the network on closed-loop system stability and performance. This approach was further developed in Nešić and Teel (2004) using a small gain analysis approach. However, the available results on network-based control have primarily utilised wired networks. In the last few years, however, several research papers have studied control using the IEEE 802.11 and Bluetooth wireless networks (see Ye, Walsh, and Bushnell (2000), Ye and Walsh (2001), Ploplys, Kawka, and Alleyne (2004), Tabbara, Nešić, and Teel (2007) and the references therein). In the design and analysis of networked control systems, the most frequently studied problem considers control over a network having constant and time-varying delays. This network behaviour is typical of communications over the Internet but does not necessarily represent the behaviour of dedicated wireless networks in which the sensor, controller and actuator nodes communicate directly with one another but might experience data losses. An appropriate framework to model lost data is the use of asynchronous systems (Ritchey and Franklin 1989; Su, Bhaya, Kaszkurewicz, and Kozyakin 1997; Hassibi, Boyd, and How 1999). In this framework, data losses occur in an stochastic manner, and the process is considered to operate in an open-loop fashion when the data is lost. The most destabilising cause of packet loss is due to bursts of poor network performance in which case large groups of packets are lost nearly consecutively. A more detailed description of bursty network performance using a two-state Markov chain was considered in Nguyen, Katz, Noble, and Satyanarayananm (1996). Modelling networks using Markov chains results in describing the overall closed-loop system as a stochastic hybrid system (Hespanha 2005). Stability results have been presented for particular cases of stochastic hybrid systems in Hassibi et al. (1999) and Mao (1999). However, these results do not directly address the problem of augmentation of dedicated, wired control systems with networked actuator and sensor devices to improve closed-loop performance.

In this work, we introduce a two-tier control architecture for nonlinear process systems with both continuous and asynchronous sensing and actuation. This class of systems arises naturally in the context of process control systems based on hybrid communication networks (i.e. point-to-point wired links integrated with network wired or wireless communication) and utilising multiple heterogeneous measurements (e.g. temperature and concentration). Assuming that there exists a lower-tier control system which relies on point-to-point communication and continuous measurements to stabilise the closed-loop system, we propose to use Lyapunov-based model predictive control (LMPC) to design an upper-tier networked control system to profit from both the continuous and the asynchronous measurements as well as from additional networked control actuators. The proposed two-tier control system architecture preserves the stability properties of the lower-tier controller while improving the closed-loop performance. The theoretical results are demonstrated using two different chemical process examples.

2. Preliminaries

2.1 *Problem formulation*

In this work, we consider nonlinear systems described by the following state-space model:

$$\begin{aligned} \dot{x}(t) &= f(x(t), u_s(t), u_a(t), w(t)) \\ y_s(t) &= h_s(x(t)) \\ y_a(t) &= h_a(x(t)), \end{aligned} \tag{1}$$

where $x(t) \in R^{n_x}$ denotes the vector of state variables, $y_s(t) \in R^{n_{ys}}$ denotes continuous and synchronous measurements, $y_a(t) \in R^{n_{ya}}$ are asynchronous and sampled measurements, $u_s(t) \in R^{n_{us}}$ and $u_a(t) \in R^{n_{ua}}$ are two different sets of possible control inputs and $w(t) \in R^{n_w}$ denotes the vector of disturbance variables. The disturbance vector is bounded, i.e. $w(t) \in W$ where

$$W := \{w \in R^{n_w} : |w| \leq \theta, \theta > 0\}.$$

$|\cdot|$ denotes Euclidean norm of a vector.

We assume that f is a locally Lipschitz vector function, h_s and h_a are sufficiently smooth functions, $f(0,0,0,0) = 0$, $h_s(0) = 0$ and $h_a(0) = 0$. This means that the origin is an equilibrium point for the nominal system (system (1) with $w(t) \equiv 0$ for all t) with $u_s(t) = 0$ and $u_a(t) = 0$.

Remark 1: The two sets of inputs include both systems with multiple inputs, or systems with a single input divided artificially into two terms; i.e.

$$\dot{x}(t) = \hat{f}(x(t), u(t), w(t))$$

with $u(t) = u_s(t) + u_a(t)$.

2.2 *Modelling of measurements and network*

System (1) is controlled using both continuous synchronous and sampled asynchronous measurements. We assume that $y_s(t)$ is available for all t, while $y_a(t)$ is sampled and only available at some time instants t_k where $\{t_{k\geq 0}\}$ is a random increasing sequence of times. We assume that the measurement of the full state $x(t_k)$ can be obtained by combining measurements $y_s(t_k)$ and $y_a(t_k)$. Due to the asynchronous nature of $y_a(t)$, the time interval between two consecutive state measurements is unknown. A controller based on the asynchronous measurements $y_a(t)$ must take into account that during consecutive state measurements, it has to operate in open loop. This class of systems arises naturally in process control, where different process variables have to be measured such as temperature, flow rate or concentration. This model is also of interest for systems controlled through a hybrid communication network in which wireless sensors are used to add redundancy to the existing working control loops (which use point-to-point wired communication links and continuous measurements) because wireless communication is often subject to data losses due to interference.

Remark 2: We have considered that the full state is available asynchronously for the controller $u_a(t)$ to simplify the notation. The results can be extended to controllers based on partial state information.

2.3 *Lower-tier controller*

The continuous measurement $y_s(t)$ can be used to design a continuous output-feedback controller to stabilise the system. We term the control system based only on the continuous measurements $y_s(t)$ as lower-tier controller. This control scheme does not use the asynchronous measurements $y_a(t)$. Figure 1 shows a schematic representation of the lower-tier controller. Following this idea, we assume that there exists an output feedback controller $u_s(t) = k_s(y_s)$ (where $k_s(y_s)$ is assumed to be a sufficiently smooth function of y_s) that renders the origin of the nominal closed-loop system (i.e. $w(t) \equiv 0$) asymptotically stable with $u_a(t) \equiv 0$. Using converse Lyapunov theorems (Khalil 1996), this assumption implies that there exist functions $\alpha_i(\cdot)$, $i = 1, 2, 3, 4$ of class $\mathcal{K}$ (class $\mathcal{K}$ functions are strictly increasing functions of their argument and satisfy $\alpha(0) = 0$) and a Lyapunov function $V(x)$ for the nominal closed-loop system which is continuous and bounded in R^{n_x}, that satisfy the following inequalities:

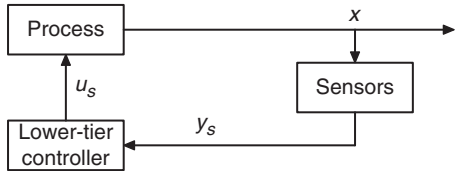

Figure 1. Lower-tier controller with dedicated point-to-point, wired communication links and continuous sensing and actuation.

$$\alpha_1(|x|) \leq V(x) \leq \alpha_2(|x|)$$

$$\frac{\partial V(x)}{\partial x} f(x, k_s(h_s(x)), 0, 0) \leq -\alpha_3(|x|)$$

$$\left| \frac{\partial V(x)}{\partial x} \right| \leq \alpha_4(|x|) \tag{2}$$

for all $x \in D \subseteq R^{n_x}$ where D is an open neighbourhood of the origin. We denote the region $\Omega_\rho \subseteq D$ (we use Ω_ρ to denote the set $\Omega_\rho := \{x \in R^{n_x} : V(x) \leq \rho\}$) as the stability region of the closed-loop system under the controller $k_s(y_s)$. In the remainder, we will refer to the controller $k_s(y_s)$ as the lower-tier controller.

The lower-tier controller $k_s(y_s)$ is able to stabilise the system; however, it does not profit from the extra information provided by $y_a(t)$. In what follows, we propose a two-tier control architecture that profits from this extra information to improve the closed-loop performance.

Remark 3: Note that in many application areas, specifically in chemical plants, there are control systems that have already been implemented using dedicated, local control networks. These control systems will not be replaced by networked control systems. Instead, networked control systems should be designed and implemented to augment the pre-existing control systems to maintain stability and improve closed-loop performance. This is why we assume that there exists a pre-existing stabilising controller $k_s(y_s)$ for the lower-tier control system based on the continuous measurements $y_s(t)$.

Remark 4: We have considered static lower-tier controllers to simplify the notation. The formulation can be extended to dynamic lower-tier controllers. In the examples given in Sections 4 and 5, proportional-integral (PI) controllers are used as the lower-tier controllers.

2.4 *Single-tier LMPC*

In order to take advantage of the asynchronous measurements, one option is to control the process using a state feedback controller that decides the input trajectories between consecutive samples. Model predictive control (MPC) is particularly appropriate for controlling systems subject to asynchronous measurements because the actuator can profit from the last-computed optimal input trajectory, to update the input when feedback is lost; the reader may refer to Mayne, Rawlings, Rao, and Scokaert (2000) and Rawlings (2000) for a tutorial and review of results on MPC. In particular, we proposed to use the LMPC design proposed in Muñoz de la Peña and Christofides (2008a) which is designed taking data losses explicitly into account, both in the optimisation problem formulation and in the controller implementation. The LMPC allows for an explicit characterisation of the stability region and guarantees that this region is an invariant set for the closed-loop system under data losses if the maximum time in which the loop is open is shorter than a given constant that depends on the parameters of the system and the Lyapunov-based controller that is used to formulate the optimisation problem. This controller is based on solving an LMPC optimisation problem that optimises both $u_s(t)$ and $u_a(t)$ when a new full state measurement is available at time step t_k. The optimal input trajectories are applied in open loop until a new full state measurement is available. This scheme does not take full advantage of the continuous measurement y_s, and applies both $u_s(t)$ and $u_a(t)$ in a sample-and-hold fashion. The LMPC controller is based on the following optimisation problem:

$$\begin{aligned}
\min_{u_a(\Delta),u_s(\Delta)} & \int_0^{\tau_f} L(\tilde{x}(\tau),u_s(\tau),u_a(\tau))\mathrm{d}\tau \\
& \dot{\tilde{x}}(\tau) = f(\tilde{x}(\tau),u_s(\tau),u_a(\tau),0) \\
& \dot{\hat{x}}(\tau) = f(\hat{x}(\tau),k_s(h_s(\hat{x}(j\Delta))),0,0) \\
& \qquad\qquad \forall \tau \in [j\Delta,(j+1)\Delta) \\
& \hat{x}(0) = \tilde{x}(0) = x(t_k) \\
& V(\tilde{x}(\tau)) \le V(\hat{x}(\tau)) \quad \forall \tau \in [0,\tau_f],
\end{aligned}$$

where $x(t_k)$ is the state obtained from both $y_s(t_k)$ and $y_a(t_k)$, $j=0,1,\ldots,$ and $\tilde{x}(\tau)$, $\hat{x}(\tau)$ are predicted trajectories of the nominal system controlled by the LMPC and the lower-tier controller applied in a sample-and-hold fashion, respectively. In the optimisation problem, $L(x,u_s,u_a)$ is a positive definite function of the state and of the inputs that define the cost and τ_f is the prediction horizon. The optimal solution to this optimisation problem is denoted as $u^*_{c,s}(\tau|t_k)$ and $u^*_{c,a}(\tau|t_k)$. These signals are defined for all $\tau \ge 0$ with $u^*_{c,s}(\tau|t_k) = u^*_{c,s}(\tau_f|t_k)$ and $u^*_{c,a}(\tau|t_k) = u^*_{c,a}(\tau_f|t_k)$ for all $\tau \ge \tau_f$.

This controller is based on the lower-tier controller $k_s(y_s)$ to design the contractive constraint (although in a sample-and-hold fashion); however, the applied control inputs $u_s(t)$ and $u_a(t)$ are not decided using the lower-tier controller, but the solution of the optimisation problem, that is

$$\begin{aligned}
u_s(t) &= u^*_{c,s}(t-t_k|t_k), \quad \forall t \in [t_k,t_{k+1}) \\
u_a(t) &= u^*_{c,a}(t-t_k|t_k), \quad \forall t \in [t_k,t_{k+1}).
\end{aligned}$$

In what follows, we denote this controller the single-tier LMPC controller. Figure 2 shows a schematic representation of this kind of state feedback control system.

3. Two-tier architecture

The main objective of the two-tier control architecture is to improve the performance of the closed-loop system using the information provided by $y_a(t)$ while guaranteeing that the stability properties of the lower-tier controller are maintained. This is done by defining a controller (upper-tier controller) based on the full state measurements obtained from both the synchronous and the asynchronous measurements at time steps t_k. In the two-tier control architecture, the upper-tier controller decides the trajectory of $u_a(t)$ between successive samples, i.e. for $t \in [t_k, t_{k+1})$ and the lower-tier controller decides $u_s(t)$ using the continuously available measurements. Figure 3 shows a schematic representation of the proposed strategy. Due to the asynchronous nature of $y_a(t)$, the upper-tier controller

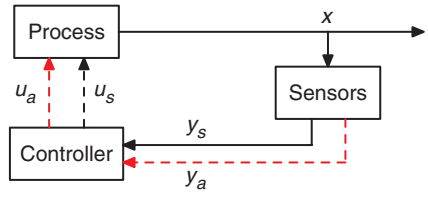

Figure 2. Centralised control system.

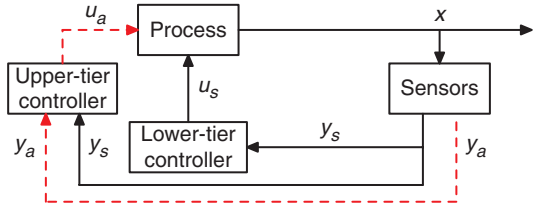

Figure 3. Two-tier control strategy (solid lines denote dedicated point-to-point, wired communication links and continuous sensing and actuation; dashed lines denote networked (wired or wireless) communication or asynchronous sampling and actuation).

has to take into account that the time interval between two consecutive samples is unknown and there exists the possibility of an infinitely large interval.

Remark 5: Note that since the lower-tier controller has already been designed, this controller views the input $u_a(t)$ as a disturbance that has to be rejected if the controller that is used to manipulate $u_a(t)$ is not properly designed. Therefore, the design of the upper-tier controller has to take into account the decisions that will be made by the lower-tier controller to maintain closed-loop stability and guarantee the improvement of the closed-loop performance.

3.1 *Upper-tier LMPC design*

In order to take advantage of the model of the system and the asynchronous state measurements, we propose to use MPC to decide $u_a(t)$. The main idea is the following: at each time instant t_k a new state measurement is obtained, an open-loop finite horizon optimal control problem is solved and an optimal input trajectory is obtained. This input trajectory is implemented until a new measurement arrives at time t_{k+1}. If the time between two consecutive measurements is longer than the prediction horizon, $u_a(t)$ is set to zero until a new measurement arrives and the optimal control problem is solved again. In order to define a finite-dimensional optimisation problem, $u_a(t)$ is constrained to the family of piece-wise constant functions with sampling period Δ, $S(\Delta)$. In order to guarantee that the resulting closed-loop system is stable, we follow a Lyapunov-based approach; see Muñoz de la Peña and Christofides (2008a). LMPC is based on including a contractive constraint that allows one to prove practical stability. In previous LMPC controllers (Mhaskar, El-Farra, and Christofides 2005, 2006; Muñoz de la Peña and Christofides 2008a), the contractive constraints are defined based on a known Lyapunov-based state feedback controller. In the present work, the contractive constraint of the proposed upper-tier LMPC design is based on the lower-tier controller. The proposed upper-tier LMPC optimisation problem is defined as follows:

$$\min_{u_a \in S(\Delta)} \int_0^{\tau_f} L(\tilde{x}(\tau), k_s(h_s(\tilde{x}(\tau))), u_a(\tau), 0)\mathrm{d}\tau \quad (3a)$$

$$\dot{\tilde{x}}(\tau) = f(\tilde{x}(\tau), k_s(h_s(\tilde{x}(\tau))), u_a(\tau), 0) \quad (3b)$$

$$\dot{\hat{x}}(\tau) = f(\hat{x}(\tau), k_s(h_s(\hat{x}(\tau))), 0, 0) \quad (3c)$$

$$\hat{x}(0) = \tilde{x}(0) = x(t_k) \quad (3d)$$

$$V(\tilde{x}(\tau)) \leq V(\hat{x}(\tau)) \quad \forall \tau \in [0, \tau_f], \quad (3e)$$

where $x(t_k)$ is the state obtained from $y_s(t_k)$ and $y_a(t_k)$, $\tilde{x}(\tau)$ is the predicted trajectory of the two-tier nominal system for the input trajectory computed by the LMPC (3), $\hat{x}(\tau)$ is the predicted trajectory of the two-tier nominal system for the input trajectory $u_a(\tau) \equiv 0$ for all $\tau \in [0, \tau_f)$. This optimisation problem does not depend on the uncertainty and assures that the system in closed-loop with the upper-tier controller maintains the stability properties of the lower-tier controller. The optimal solution to this optimisation problem is denoted as $u^*_{u,a}(\tau|t_k)$. This signal is defined for all $\tau \geq 0$ with $u^*_{u,a}(\tau|t_k) = 0$ for all $\tau \geq \tau_f$.

The control inputs of the proposed two-tier control architecture based on the above-mentioned LMPC are defined as follows:

$$\begin{aligned} u_s(t) &= k_s(h_s(x(t))), \ \forall t \\ u_a(t) &= u^*_{u,a}(t - t_k|t_k), \ \forall t \in [t_k, t_{k+1}) \end{aligned} \quad (4)$$

where $u^*_{u,a}(t - t_k|t_k)$, is the optimal solution of the LMPC optimisation problem (3) at time step t_k. This implementation technique takes into account that the lower-tier controller uses the continuously available measurements, while the upper-tier controller has to operate in open loop between consecutive asynchronous measurements.

Note that the constraint (3e) in the LMPC (3) is needed to ensure that the value of the Lyapunov function of the closed-loop system under the proposed two-tier control architecture (4) is lower than or equal to the Lyapunov function of the closed-loop system when it is only controlled by the lower-tier controller. By imposing constraint (3e), we can prove the stability of the closed-loop system under the two-tier control architecture (4) which is shown in Section 3.2.

Remark 6: By definition, $u^*_a(\tau|t_k) = 0$ for all $\tau \geq \tau_f$. This implies that the upper-tier controller switches off when it has been operating in open loop for a large time, because in this case, the last received information is no longer useful to improve the performance of the lower-tier controller. The two-tier control architecture is (by design) stable because of the lower-tier controller stability properties. The main problem is how to improve the closed-loop performance using non-reliable communications in a way such that the stability properties of the closed-loop system under the lower-tier controller are not compromised. Setting the control input of the upper-tier controller to zero after a given time is necessary to maintain the stability properties, because after a sufficiently large time, the upper-tier input implemented in open loop is not improving the closed loop performance and may act as a disturbance.

Remark 7: State and input constraints are beyond the scope of this work; however, the results can be extended as in previous LMPC results (Mhaskar et al. 2005, 2006; Muñoz de la Peña and Christofides 2008a).

3.2 *Two-tier controller stability*

Combining the information from a hybrid communication system may lead to losing the stability properties of the lower-tier controller. The resulting closed-loop system is an asynchronous system and studying the stability of this class of systems is in general a difficult task (Muñoz de la Peña and Christofides 2008b). This implies that the design of the upper-tier controller is also a difficult task. In this work, we propose to follow a Lyapunov-based approach. The main idea is to compute the input $u_a(t)$ applied to the system in a way such that it is guaranteed that the value of the Lyapunov function at time steps t_k, $V(x(t_k))$, is a decreasing sequence of values with a lower bound. This guarantees the practical stability of the closed-loop system. This is achieved due to the contractive constraint (3e) of LMPC (3). This property is presented in Theorem 1 below. To state this theorem, we need the following propositions.

Proposition 1 (cf. Khalil 1996)**:** *Consider system* (1) *in closed-loop with the lower-tier controller k_s. Taking into account* (2)*, there exists a $\mathcal{KL}$ (function $\beta(r,s)$* is *said to be a class $\mathcal{KL}$ function if, for each fixed s, $\beta(r,s)$ belongs to class $\mathcal{K}$ function with respect to r and, for each fixed r, $\beta(r,s)$ is decreasing with respect to s and $\beta(r,s)\to 0$ as $s\to 0$) function $\beta(r,s)$, a $\mathcal{K}$ function γ and a constant $\theta_{\max}$ such that if $x(t_0)\in\Omega_\rho$ and $u_a(t)=0$ for all t, then*

$$V(x(t)) \le \beta(V(x(t_0)), t-t_0) + \gamma(\max_{\tau\in[t_0,t]}|w(\tau)|)$$

for all $w\in W$ with $\theta\le\theta_{\max}$.

This proposition provides us with a bound on the trajectories of the Lyapunov function of the state of the system in closed loop with the lower-tier controller with $u_a(t)=0$. We will use this bound to prove the stability theorem.

Proposition 2: *Consider the following state trajectories*:

$$\begin{aligned}\dot{x}_a(t) &= f(x_a(t), k_s(h_s(x_a(t))), u_a(t), w(t))\\ \dot{x}_b(t) &= f(x_b(t), k_s(h_s(x_b(t))), u_a(t), 0)\end{aligned} \tag{5}$$

with initial states $x_a(t_0)=x_b(t_0)\in\Omega_\rho$. There exists a class $\mathcal{K}$ function f_W such that

$$|x_a(t)-x_b(t)| \le f_W(t-t_0) \tag{6}$$

for all $x_a(t)$, $x_b(t)\in\Omega_\rho$ and all $w(t)\in W$.

Proof: Define the error vector as $e(t)=x_a(t)-x_b(t)$. The time derivative of the error is given by

$$\begin{aligned}\dot{e}(t) = {} & f(x_a(t), k_s(h_s(x_a(t))), u_a(t), w(t))\\ & - f(x_b(t), k_s(h_s(x_b(t))), u_a(t), 0).\end{aligned}$$

By continuity and the local Lipschitz property assumed for the vector field $f(x,u_s,u_a,w)$, there exist positive constants L_w, L_x and L_{u1} such that

$$\begin{aligned}|\dot{e}(t)| \le {} & L_w|w(t)-0| + L_x|x_a(t)-x_b(t)|\\ & + L_{u1}|k_s(h_s(x_a(t))) - k_s(h_s(x_b(t)))|\end{aligned} \tag{7}$$

for all $x_a(t)$, $x_b(t)\in\Omega_\rho$ and $w(t)\in W$. By continuity and smooth properties of k_s and h_s, there exists a positive constant L_{u2} such that

$$|k_s(h_s(x_a(t))) - k_s(h_s(x_b(t)))| \le L_{u2}|x_a(t)-x_b(t)|$$

for all $x_a(t)$, $x_b(t)\in\Omega_\rho$. Thus the following inequality can be obtained from inequality (7):

$$\begin{aligned}|\dot{e}(t)| &\le L_w|w(t)| + (L_x + L_{u1}L_{u2})|x_a(t)-x_b(t)|\\ &\le L_w\theta + (L_x + L_{u1}L_{u2})|e(t)|.\end{aligned}$$

Integrating $|\dot{e}(t)|$ with initial condition $e(t_0)=0$ (recall that $x_a(t_0)=x_b(t_0)$), the following bound on the norm of the error vector is obtained:

$$|e(t)| \le \frac{L_w\theta}{L'_x}(e^{L'_x(t-t_0)}-1),$$

where $L'_x = L_x + L_{u1}L_{u2}$. This implies that (6) holds for

$$f_W(\tau) = \frac{L_w\theta}{L'_x}(e^{L'_x\tau}-1).$$

□

The following proposition bounds the difference between the magnitudes of the Lyapunov function of two different states in Ω_ρ.

Proposition 3: *Consider the Lyapunov function $V(\cdot)$ of system* (1)*. There exists a quadratic function $f_V(\cdot)$ such that*

$$V(x) \le V(\hat{x}) + f_V(|x-\hat{x}|) \tag{8}$$

for all $x,\hat{x}\in\Omega_\rho$.

Proof: Because the Lyapunov function $V(x)$ is continuous and bounded on compact sets, we can find a positive constant M such that a Taylor series expansion of V around $\hat{x}$ yields

$$V(x) \le V(\hat{x}) + \frac{\partial V}{\partial x}|x-\hat{x}| + M|x-\hat{x}|^2, \quad \forall x,\hat{x}\in\Omega_\rho.$$

Note that the term $M|x-\hat{x}|^2$ bounds the high-order terms of the Taylor series of $V(x)$ for all $x,\hat{x}\in\Omega_\rho$. Taking into account (2), the following bound for $V(x)$ is obtained:

$$V(x) \le V(\hat{x}) + \alpha_4(\alpha_1^{-1}(\rho))|x-\hat{x}| + M|x-\hat{x}|^2, \ \forall x,\hat{x}\in\Omega_\rho.$$

This implies that (8) holds for $f_V(x) = \alpha_4(\alpha_1^{-1}(\rho))x + Mx^2$. □

Theorem 1: *Consider system* (1) *in closed-loop with the two-tier control architecture* (4). *If* $x(t_0) \in \Omega_\rho$, $\theta \leq \theta_{\max}$, *and there exist a concave function g such that*

$$g(x) \geq \beta(x, \tau_f) \tag{9}$$

for all $x \in \Omega_\rho$, *and a positive constant* $c \leq \rho$ *such that*

$$c - g(c) \geq f_V(f_W(\tau_f)), \tag{10}$$

then $x(t)$ *is ultimately bounded in a region that contains the origin.*

Proof: In order to prove that the closed-loop system is ultimately bounded in a region that contains the origin, we will prove that $V(x(t_k))$ is a decreasing sequence of values with a lower bound for the worst possible case, that is, the upper-tier controller always operates in open loop for a period of time longer than τ_f between consecutive samples, that is, $t_{k+1} - t_k > \tau_f$ for all k. The trajectory $\hat{x}(t)$ corresponds to the nominal system in closed loop with the lower-tier controller with initial state $x(t_k)$. Taking into account Proposition 1 the following inequality holds:

$$V(\hat{x}(t)) \leq \beta(V(x(t_k)), t - t_k).$$

The contractive constraint (3e) of the proposed LMPC (3) guarantees that

$$V(\tilde{x}(t)) \leq V(\hat{x}(t)), \quad \forall t \in [t_k, t_k + \tau_f].$$

Assuming that $x(t) \in \Omega_\rho$ for all times (which is automatically satisfied when the system is proved to be ultimately bounded below), we can apply Proposition 3 to obtain the following inequalities:

$$V(x(t_k + \tau_f)) \leq V(\tilde{x}(t_k + \tau_f)) + f_V(|x(t_k) - \tilde{x}(t_k)|).$$

Applying Proposition 2 we obtain the following upper bounds on the deviation of $\tilde{x}(t)$ from $x(t)$:

$$|x(t_k + \tau_f) - \tilde{x}(t_k + \tau_f)| \leq f_W(\tau_f).$$

Using the above inequalities the following upper bound on $V(x(t_k + \tau_f))$ is obtained:

$$V(x(t_k + \tau_f)) \leq \beta(V(x(t_k)), \tau_f) + f_V(f_W(\tau_f)). \tag{11}$$

Taking into account that for all $t > t_k + \tau_f$ the upper-tier controller is switched off, i.e. $u_a(t) = 0$, and only the lower-tier controller is in action, the following bound on $V(x(t_{k+1}))$ is obtained from Proposition 1:

$$V(x(t_{k+1})) \leq \max\{V(x(t_k + \tau_f)), \gamma(\theta_{\max})\}$$

for all $w(t) \in W$. Because function g is concave, $z - g(z)$ is an increasing function. If there is a positive constant $c \leq \rho$ satisfying (10), then (10) holds for all $z > c$. Taking into account that $g(z) \geq \beta(z, \tau_f)$ for all $z \leq \rho$, the following inequality is obtained:

$$z - \beta(z, \tau_f) \geq f_V(f_W(\tau_f))$$

when $c \leq z \leq \rho$. From this inequality and inequality (11), we obtain that

$$V(x(t_{k+1})) \leq \max\{V(x(t_k)), \gamma(\theta_{\max})\}$$

for all $V(x(t_k)) \geq c$. It follows using Lyapunov arguments that

$$\limsup_{t \to \infty} V(x(t)) \leq \rho_c,$$

where

$$\rho_c = \max\{\max_c \beta(c, \tau_f) + f_V(f_W(\tau_f)), \gamma(\theta_{\max})\}. \quad \square$$

Remark 8: In general, the size of the region in which the state is ultimately bounded depends on the prediction horizon τ_f. The prediction horizon τ_f sets the maximum amount of time on which the upper-tier controller will be operating in open loop.

Remark 9: Although the proof of Theorem 1 is constructive, the constants obtained are conservative. This is the case with most of the results of the type presented in this article. In practice, the maximum time that the upper-tier controller should operate in open loop is better estimated through closed-loop simulations. The various inequalities provided are more useful as guidelines on the interaction between the various parameters that define the system and the upper-tier controller and may be used as guidelines to design the controller and the network; see, for example, Nešić, Teel, and Kokotovic (1999) and Tabuada and Wang (2006) for further discussion on this issue.

Remark 10: Referring to Theorem 1, the assumption that there exists a concave function g such that $g(x) \geq \beta(x, \tau_f)$ imposes an upper bound on τ_f and is made, without any loss of generality, to simplify the proof of Theorem 1; i.e. the result of Theorem 1 could still be proved without this assumption but the proof would be more involved. The assumption that there exists a positive constant $c \leq \rho$ such that $c - g(c) \geq f_V(f_W(\tau_f))$ guarantees that the derivative of the Lyapunov function of the state of the closed-loop system outside the level set $V(x) = c$ is negative under the two-tier control architecture with the upper-tier LMPC (3).

Remark 11: As in all MPC schemes, it is not possible to provide quantitative results that guarantee that the performance of the closed-loop system is better than any other controller, unless an infinite horizon is used. It makes sense that the system in closed loop with the two-tier control architecture has, in general, a better performance because the cost function is taken into

account in the optimisation problem of the upper-tier controller. The case studies provide results that demonstrate this point.

4. Application to a chemical reactor

Consider a well-mixed, non-isothermal continuous stirred tank reactor where three parallel irreversible elementary exothermic reactions take place of the form $A \to B$, $A \to C$ and $A \to D$. The product B is the desired product and C and D are byproducts. The feed to the reactor consists of A at temperature T_{A0} and concentration C_{A0} and flow rate $F+\Delta F$, where ΔF is a time-varying uncertainty. Due to the non-isothermal nature of the reactor, a jacket is used to remove or provide heat from or to the reactor. Using first principles and standard modelling assumptions the following mathematical model of the process is obtained:

$$\begin{aligned}\frac{\mathrm{d}T}{\mathrm{d}t} &= \frac{F+\Delta F}{V_r}(T_{A0}-T) - \sum_{i=1}^{3}\frac{\Delta H_i}{\rho C_p}k_{i0}e^{\frac{-E_i}{RT}}C_A + \frac{Q}{\rho C_p V_r}\\ \frac{\mathrm{d}C_A}{\mathrm{d}t} &= \frac{F+\Delta F}{V_r}(C_{A0}-C_A+\Delta C_{A0}) + \sum_{i=1}^{3}k_{i0}e^{\frac{-E_i}{RT}}C_A,\end{aligned} \tag{12}$$

where C_A denotes the concentration of the reactant A, T denotes the temperature of the reactor, V_r denotes the volume of the reactor, ΔH_i, k_{i0}, E_i, $i=1,2,3$ denote the enthalpies, pre-exponential constants and activation energies of the three reactions, respectively, and C_p and ρ denote the heat capacity and the density of the fluid in the reactor. The inputs to the system are the rate of heat input or removal Q and the change of the inlet reactant A at concentration ΔC_{A0}. The values of the process parameters are shown in Table 1.

System (12) has three steady states (two locally asymptotically stable and one unstable). The control objective is to stabilise the system at the open-loop unstable steady state $T_s = 388\,\mathrm{K}$, $C_{As} = 3.59\,\mathrm{mol/l}$. The flow rate uncertainty is bounded by $|\Delta F| \le 3\,\mathrm{m}^3/\mathrm{h}$.

We assume that the measurements of temperature T are available continuously, and the measurements of the concentration C_A are available asynchronously at time instants $\{t_{k\ge 0}\}$. We also assume that there exists a lower bound $\Delta_{\min}$ on the time interval between two consecutive concentration measurements.

In order to model the time sequence $\{t_{k\ge 0}\}$, we use a lower-bounded random Poisson process. The Poisson process is defined by the number of events per unit time W. The interval between two consecutive concentration sampling times (events of the Poisson process) is given by $\Delta_a = \max\{\Delta_{\min}, \frac{-\ln\chi}{W}\}$, where χ is a random variable with uniform probability distribution between 0 and 1. For the simulations carried out in this work we pick $\Delta_{\min} = 0.025\,\mathrm{h}$, which is meaningful from a practical point of view with respect to concentration measurements.

Table 1. Process parameters.

F	$4.998\ (\mathrm{m}^3/\mathrm{h})$	k_{10}	$3\times10^6\,(\mathrm{h}^{-1})$
V_r	$1(\mathrm{m}^3)$	k_{20}	$3\times10^5\,(\mathrm{h}^{-1})$
R	$8.314\,(\mathrm{KJ/kmol\,K})$	k_{30}	$3\times10^5\,(\mathrm{h}^{-1})$
T_{A0}	$300\,(\mathrm{K})$	E_1	$5\times10^4\,(\mathrm{KJ/kmol})$
C_{A0s}	$4\ (\mathrm{kmol/m}^3)$	E_2	$7.53\times10^4\,(\mathrm{KJ/kmol})$
ΔH_1	$-5.0\times10^4\,(\mathrm{KJ/kmol})$	E_3	$7.53\times10^4\,(\mathrm{KJ/kmol})$
ΔH_2	$-5.2\times10^4\,(\mathrm{KJ/kmol})$	ρ	$1000\,(\mathrm{kg/m}^3)$
ΔH_3	$-5.4\times10^4\,(\mathrm{KJ/kmol})$	C_p	$0.231\,(\mathrm{KJ/kg\,K})$

The process model (12) belongs to the class of nonlinear systems described by system (1) where $x^T = [x_1\ x_2] = [T - T_s\ C_A - C_{As}]$ is the state, $u_s = Q$ and $u_a = \Delta C_{A0}$ are the manipulated inputs, $w = \Delta F$ is a time varying bounded disturbance, $y_s = x_1 = T - T_s$ is obtained from the continuous temperature measurement T and $y_a = x_2 = C_A - C_{As}$ is obtained from the asynchronously sampled concentration measurement C_A.

First, an output feedback controller (lower-tier controller) based on the continuous temperature measurements (i.e. x_1) is designed to stabilise system (12) using only the rate of heat input $u_s = Q$ as the manipulated input, which is bounded by $|u_s| \le 10^5\,\mathrm{KJ/h}$. In particular, the following PI control law is used as the lower-tier controller:

$$u_s(t) = K\left(x_1(t) + \frac{1}{T_i}\int_0^t x_1(\tau)\mathrm{d}\tau\right), \tag{13}$$

where K is the proportional gain and T_i is the integral time constant. To compute the parameters of the PI controller, the linearised model $\dot{x} = Ax + Bu_s$ of system (12) around the equilibrium point is obtained. The proportional gain K is chosen to be -8100. This value guarantees that the origin of $\dot{x} = (A + BK[1\ 0])x$ is asymptotically stable with its eigenvalues being $\lambda_1 = -1.06\times10^5$ and $\lambda_2 = -4.43$. A quadratic Lyapunov function $V(x) = x^T P x$ with

$$P = \begin{bmatrix} 0.024 & 5.21 \\ 5.21 & 1.13\times10^3 \end{bmatrix}$$

is obtained by solving an algebraic Lyapunov equation $A_c^T P + PA_c + Q_c = 0$ for P with $A_c = A + BK[1\ 0]$. This Lyapunov function will be used to design the upper-tier LMPC and the single-tier LMPC. The integral time constant is chosen to be $T_i = 49.6\,\mathrm{h}$. For simplicity, the Lyapunov function $V(x)$ is determined on the basis of the closed-loop system under the proportional (P) term of the PI controller only; the effect of the integral (I) term is very small for the

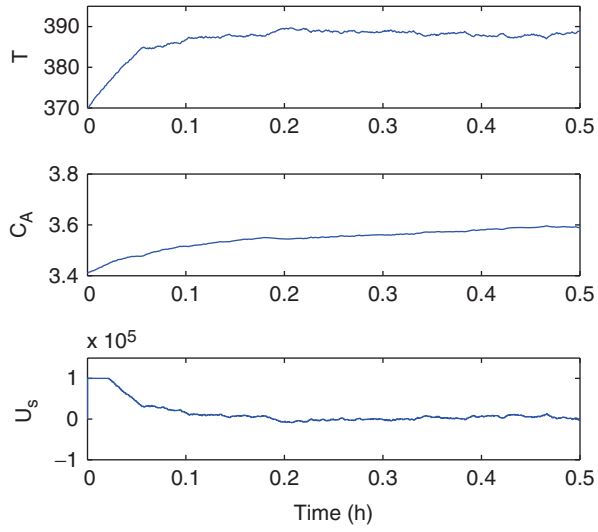

Figure 4. State and input trajectories of system (12) under lower-tier PI control (13).

specific choice of the controller parameters used in the simulations. The state and input trajectories of system (12) starting from $x_0 = [370 \;\; 3.41]^T$ under the PI controller are shown in Figure 4. From Figure 4, we see that the PI controller (13) stabilises the temperature and concentration of system (12) at the equilibrium point in about 0.1 and 0.2 h, respectively.

Next, we implemented the proposed two-tier control architecture to improve the performance of the closed-loop system. In this set of simulations, the PI controller (13) is used as the lower-tier controller. Instead of abandoning the less frequent concentration measurement, we take advantage of both the continuous measurements of the temperature T and the asynchronous concentration measurements C_A together with the nominal model of system (12) to design the upper-tier LMPC. The inlet concentration change ΔC_{A0}, which is bounded by $|\Delta C_{A0}| \leq 1\,\text{kmol/m}^3$, is the manipulated input for the upper-tier LMPC. In the design of the upper-tier LMPC, the performance index is defined by the following positive definite function:

$$L(x, u_s, u_a) = x^T Q_c x, \tag{14}$$

where x is the state of the system and Q_c is the following weight matrix:

$$Q_c = \begin{bmatrix} 1 & 0 \\ 0 & 10^4 \end{bmatrix}.$$

The values of the weights in Q_c have been chosen to account for the different range of numerical values for each state. The sampling time of the LMPC is $\Delta = 0.025$ h; the prediction horizon is $\tau_f = 11\Delta$ so that the prediction captures most of the dynamic evolution of the process.

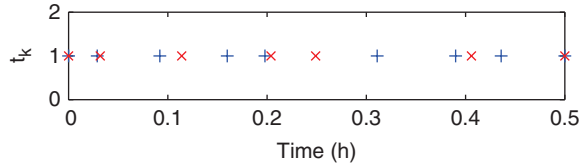

Figure 5. Concentration sampling times, +: sampling times generated with $W = 30$, {×}: sampling times generated with $W = 20$.

The two-tier control architecture is implemented as discussed in the previous section. The lower-tier controller uses the continuous temperature measurements to control $u_s(t)$. When the measurements of T and C_A are obtained at time instant t_k, an estimate of the state of system (12), $x_e(t_k)$, is obtained from the two measurements at t_k. Based on the estimated state $x_e(t_k)$, the LMPC optimisation problem (3) is solved and an optimal input trajectory $u^*_{u,a}(\tau|t_k)$ is obtained. This optimal input trajectory is implemented until a new concentration measurement is obtained at time t_{k+1} (note that k indexes the number of concentration samples received, not a given sampling time). Note that because a PI controller is used in the lower tier, we need to predict the controller dynamics (the control effects generated by the integral part) in the optimisation problem of the proposed LMPC scheme (3).

The stability and robustness of the two-tier control architecture (4) have been studied with two different initial conditions $x(0) = [370 \;\; 3.41]^T$ and $x(0) = [375 \;\; 3.46]^T$ associated with two different concentrations measurement sequences $\{t_{k\geq 0}\}$ (Figure 5) generated with $W = 30$ and $W = 20$, respectively. The average time intervals between two consecutive sampling times are 0.0625 h for $W = 30$ and 0.0833 h for $W = 20$. In addition, two different disturbance trajectories of $w(t)$ with a random value at each simulation step are added to the closed-loop system. The state and inputs trajectories of system (12) under the proposed two-tier control architecture are shown in Figure 6. From Figure 6, we see that the two-tier control architecture (4) stabilises the temperature and concentration of the system in about 0.1 and 0.05 h respectively. This implies that the resulting closed-loop system response is faster. Moreover, the cost associated with the resulting closed-loop trajectories is lower.

Moreover, another set of simulations was carried out to compare the proposed two-tier control architecture with the lower-tier PI control system from a performance index point of view. Table 2 shows the total cost computed for 20 different closed-loop simulations under the proposed two-tier control architecture and the PI control scheme. To carry out this comparison, we have computed the total cost of each simulation based on the integral of the performance

index defined by $L(x, u_s, u_a)$ from the initial time to the end of the simulation $t_f = 0.5$ h. For this set of simulations W is chosen to be 10. For each pair of simulations (one for each control scheme) a different initial state inside the stability region, a different uncertainty trajectory and a different random concentration measurement sequence are chosen. As can be seen in Table 2, the proposed two-tier control architecture has a cost lower than the corresponding total cost under the PI controller in all the simulations.

We have also carried out another set of simulations to compare the proposed two-tier scheme with a controller using the measurements of T and C_A to decide both control inputs u_s and u_a in the single-tier LMPC framework; see Section 2.4. This implies that this approach does not take full advantage of the continuous measurement of T. The LMPC optimises the future sampled input trajectory $u_a(t)$, $u_s(t)$ with sampling time Δ. When at a time instant t_k, both the measurements of T and C_A are available (an estimate of the state is available), this optimisation problem is evaluated and two optimal input trajectories $u^*_{c,s}(\tau|t_k)$ and $u^*_{c,a}(\tau|t_k)$ are obtained and implemented until the next measurement of both T and C_A are available.

For these simulations, the single-tier LMPC uses the same parameters as the ones of the two-tier controller. The same initial conditions, concentration sampling times (Figure 5) and disturbance trajectories are used in this set of simulations. The state and inputs trajectories of the closed-loop system under the LMPC scheme are shown in Figure 7. From Figure 7, it can be seen that the single-tier LMPC stabilises the system (solid curves) when the time intervals between two consecutive measurements are small (0.0625 h on average), but loses stability and cannot stabilise the system (dashed curves) when these time intervals get bigger (0.0833 h on average). The single-tier LMPC does not profit from the continuous measurements of the temperature, thus, the stability region of the closed-loop system is, in general, reduced to a much smaller one compared to that obtained under the two-tier control architecture.

Table 2. Total performance cost along the closed-loop trajectories.

Sim.	Two-tier	PI controller	Sim.	Two-tier	PI controller
1	203.92	704.54	11	224.03	831.63
2	188.74	815.47	12	203.78	738.47
3	198.33	922.87	13	265.44	617.15
4	221.76	640.87	14	210.58	704.95
5	240.44	656.47	15	190.68	723.05
6	226.44	847.43	16	209.66	695.60
7	199.19	779.03	17	205.90	808.71
8	233.40	736.65	18	211.29	749.24
9	200.45	702.26	19	214.79	737.62
10	198.74	753.25	20	217.13	813.70

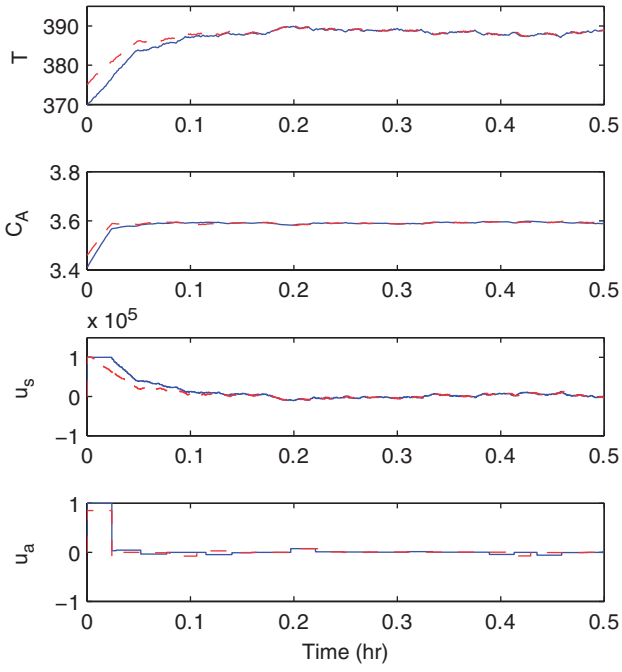

Figure 6. State and inputs trajectories of system (12) under the proposed two-tier control architecture when $W = 30$ (solid curves) and $W = 20$ (dashed curves).

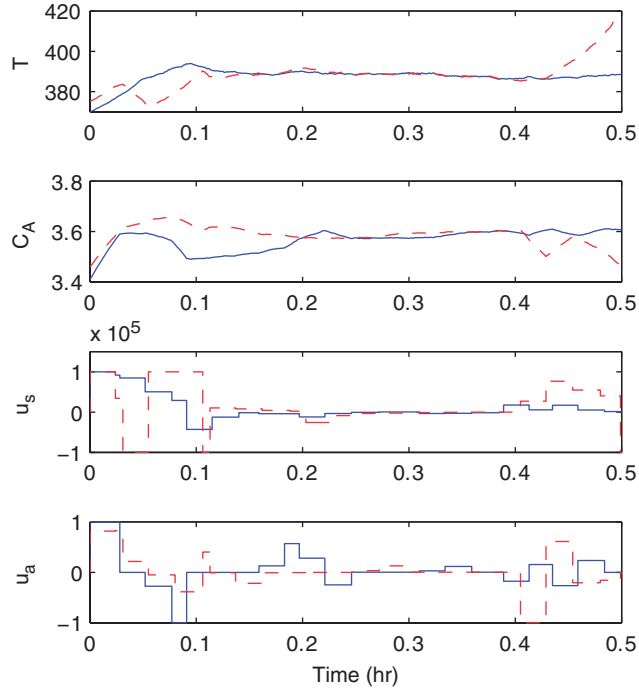

Figure 7. State and inputs trajectories of system (12) under the single-tier LMPC scheme with concentration sampling times generated with $W = 30$ (solid curves) and $W = 20$ (dashed curves).

5. Application to a reactor–separator process

The process considered in this example is a three vessel reactor–separator system consisting of two continuously stirred tank reactors (CSTRs) and a flash tank separator (Figure 8). A feed stream to the first CSTR F_{10} contains the reactant A which is converted into the desired product B. The desired product B can then further react into an undesired side-product C. The effluent of the first CSTR along with additional fresh feed F_{20} makes up the inlet to the second CSTR. The reactions $A \rightarrow B$ and $B \rightarrow C$ (referred to as 1 and 2, respectively) take place in the two CSTRs in series before the effluent from CSTR 2 is fed to a flash tank. The overhead vapour from the flash tank is condensed and recycled to the first CSTR, and the bottom product stream is removed. A small portion of the overhead is purged before being recycled to the first CSTR. All the three vessels are assumed to have static holdup. The dynamic equations describing the behaviour of the system, obtained through material and energy balances under standard modelling assumptions, are given below.

$$
\begin{aligned}
\frac{dx_{A1}}{dt} &= \frac{F_{10}}{V_1}(x_{A10} - x_{A1}) + \frac{F_r}{V_1}(x_{Ar} - x_{A1}) - k_1 e^{\frac{-E_1}{RT_1}} x_{A1} \\
\frac{dx_{B1}}{dt} &= \frac{F_{10}}{V_1}(x_{B10} - x_{B1}) + \frac{F_r}{V_1}(x_{Br} - x_{B1}) \\
&\quad + k_1 e^{\frac{-E_1}{RT_1}} x_{A1} - k_2 e^{\frac{-E_2}{RT_1}} x_{B1} \\
\frac{dT_1}{dt} &= \frac{F_{10}}{V_1}(T_{10} - T_1) + \frac{F_r}{V_1}(T_3 - T_1) + \frac{-\Delta H_1}{C_p} k_1 e^{\frac{-E_1}{RT_1}} x_{A1} \\
&\quad + \frac{-\Delta H_2}{C_p} k_2 e^{\frac{-E_2}{RT_1}} x_{B1} + \frac{Q_1}{\rho C_p V_1} \\
\frac{dx_{A2}}{dt} &= \frac{F_1}{V_2}(x_{A1} - x_{A2}) + \frac{F_{20}}{V_2}(x_{A20} - x_{A2}) - k_1 e^{\frac{-E_1}{RT_2}} x_{A2} \\
\frac{dx_{B2}}{dt} &= \frac{F_1}{V_2}(x_{B1} - x_{B2}) + \frac{F_{20}}{V_2}(x_{B20} - x_{B2}) \\
&\quad + k_1 e^{\frac{-E_1}{RT_2}} x_{A2} - k_2 e^{\frac{-E_2}{RT_2}} x_{B2} \\
\frac{dT_2}{dt} &= \frac{F_1}{V_2}(T_1 - T_2) + \frac{F_{20}}{V_2}(T_{20} - T_2) + \frac{-\Delta H_1}{C_p} k_1 e^{\frac{-E_1}{RT_2}} x_{A2} \\
&\quad + \frac{-\Delta H_2}{C_p} k_2 e^{\frac{-E_2}{RT_2}} x_{B2} + \frac{Q_2}{\rho C_p V_2} \\
\frac{dx_{A3}}{dt} &= \frac{F_2}{V_3}(x_{A2} - x_{A3}) - \frac{F_r + F_p}{V_3}(x_{Ar} - x_{A3}) \\
\frac{dx_{B3}}{dt} &= \frac{F_2}{V_3}(x_{B2} - x_{B3}) - \frac{F_r + F_p}{V_3}(x_{Br} - x_{B3}) \\
\frac{dT_3}{dt} &= \frac{F_2}{V_3}(T_2 - T_3) + \frac{Q_3}{\rho C_p V_3}.
\end{aligned} \tag{15}
$$

The model of the flash tank separator operates under the assumption that the relative volatility for each of the species remains constant within the operating temperature range of the flash tank. This assumption allows calculating the mass fractions in the overhead based upon the mass fractions in the liquid portion of the vessel. It has also been assumed that there is a negligible amount of reaction taking place in the separator. The following algebraic equations model the composition of the overhead stream relative to the composition of the liquid holdup in the flash tank:

$$
\begin{aligned}
x_{Ar} &= \frac{\alpha_A x_{A3}}{\alpha_A x_{A3} + \alpha_B x_{B3} + \alpha_C x_{C3}} \\
x_{Br} &= \frac{\alpha_B x_{B3}}{\alpha_A x_{A3} + \alpha_B x_{B3} + \alpha_C x_{C3}} \\
x_{Cr} &= \frac{\alpha_C x_{C3}}{\alpha_A x_{A3} + \alpha_B x_{B3} + \alpha_C x_{C3}}.
\end{aligned} \tag{16}
$$

The definitions for the variables used in (15) can be found in Table 3, with the parameter values given in Table 4.

Each of the tanks has an external heat input. The manipulated inputs to the system are the heat inputs to the three vessels, Q_1, Q_2 and Q_3, and the feed stream flow rate to vessel 2, F_{20}.

We assume that the measurements of temperatures T_1, T_2 and T_3 are available continuously, and the

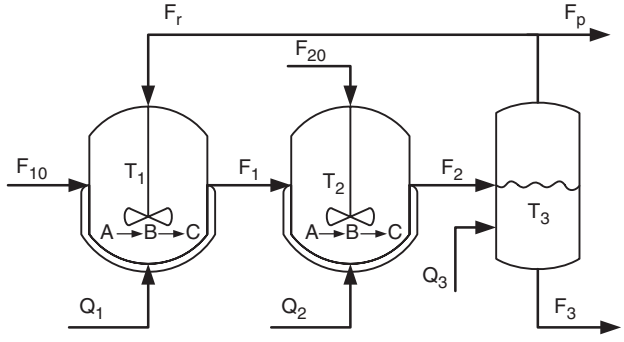

Figure 8. Reactor–separator system with recycle.

Table 3. Process variables.

x_{A1}, x_{A2}, x_{A3}	Mass fractions of A in vessels 1, 2, 3
x_{B1}, x_{B2}, x_{B3}	Mass fractions of B in vessels 1, 2, 3
x_{C1}, x_{C2}, x_{C3}	Mass fractions of C in vessels 1, 2, 3
x_{Ar}, x_{Br}, x_{Cr}	Mass fractions of A, B, C in the recycle
T_1, T_2, T_3	Temperatures in vessels 1, 2, 3
T_{10}, T_{20}	Feed stream temperatures to vessels 1, 2
F_1, F_2	Effluent flow rate from vessels 1, 2
F_{10}, F_{20}	Feed stream flow rates to vessels 1, 2
F_r, F_p	Flow rates of the recycle and purge
V_1, V_2, V_3	Volumes of vessels 1, 2, 3
E_1, E_2	Activation energy for reactions 1, 2
k_1, k_2	Pre-exponential values for reactions 1, 2
ΔH_1, ΔH_2	Heats of reaction for reactions 1, 2
α_A, α_B, α_C	Relative volatilities of A, B, C
Q_1, Q_2, Q_3	Heat inputs into vessels 1, 2, 3
C_p, R, ρ	Heat capacity, gas constant and solution density

Table 4. Process parameters.

T_{10}	300 (K)	k_1	$2.77 \times 10^3\,(s^{-1})$
T_{20}	300 (K)	k_2	$2.5 \times 10^3\,(s^{-1})$
F_{10}	5.04 (m^3/h)	ΔH_1	-6×10^4 (KJ/kmol)
F_r	50.4 (m^3/h)	ΔH_2	-7×10^4 (KJ/kmol)
F_p	5.04 (m^3/h)	α_A	3.5
V_1	1.0 (m^3)	α_B	1
V_2	0.5 (m^3)	α_C	0.5
V_3	1.0 (m^3)	C_p	4.2 [KJ/kg K]
E_1	5×10^4 (KJ/kmol)	R	8.314 (KJ/kmol K)
E_2	6×10^4 (KJ/kmol)	ρ	1000 (kg/m^3)

Table 5. Steady-state operation parameters of x_{s1} and x_{s2}.

	x_{s1}		x_{s2}
Q_{1s}	12.6×10^5 (KJ/h)	Q_{1s}	12.6×10^5 (KJ/h)
Q_{2s}	16.2×10^5 (KJ/h)	Q_{2s}	13.32×10^5 (KJ/h)
Q_{3s}	12.6×10^5 (KJ/h)	Q_{3s}	11.88×10^5 (KJ/h)
F_{20s}	5.04 (m^3/h)	F_{20s}	5.04 (m^3/h)

Table 6. Steady states x_{s1} and x_{s2}.

	x_{A1s}	x_{B1s}	T_{1s}	x_{A2s}	x_{B2s}	T_{2s}	x_{A3s}	x_{B3s}	T_{3s}
x_{s1}	0.383	0.581	447.8	0.391	0.572	444.6	0.172	0.748	449.6
x_{s2}	0.605	0.386	425.9	0.605	0.386	422.6	0.346	0.630	427.3

measurements of mass fractions x_{A1}, x_{B1}, x_{A2}, x_{B2}, x_{A3} and x_{B3} are available asynchronously at time instants $\{t_{k\geq0}\}$. The same method used in the example in Section 4 is used in this example to generate the time sequence $\{t_{k\geq0}\}$.

For each set of steady-state inputs Q_{1s}, Q_{2s}, Q_{3s} and F_{20s} corresponding to a different operation condition, system (15) has one stable steady state x_s^T. In this example, we will study two different operating conditions corresponding to two different steady states x_{s1} and x_{s2}. The parameters of the steady-state operation points and the values of the two steady states are given in Tables 5 and 6. The control objective is to steer the system to the steady states from the initial state

$$x(0)^T = [0.890\ 0.110\ 388.732\ 0.886\ 0.113\ 386.318\ 0.748\ 0.251\ 390.570].$$

The process model (15) belongs to the class of nonlinear systems described by system (1) where $x^T = [x_1\,x_2\,x_3\,x_4\,x_5\,x_6\,x_7\,x_8\,x_9] = [x_{A1} - x_{A1s}\ x_{B1} - x_{B1s}\ T_1 - T_{1s}\ x_{A2} - x_{A2s}\ x_{B2} - x_{B2s}\ \ T_2 - T_{2s}\ x_{A3} - x_{A3s}\ \ x_{B3} - x_{B3s}\ T_3 - T_{3s}]$ is the state, $u_s^T = [u_{s1}\,u_{s2}\,u_{s3}] = [Q_1 - Q_{1s}\ Q_2 - Q_{2s}\ Q_3 - Q_{3s}]$ and $u_a = F_{20} - F_{20s}$ are the manipulated inputs, $y_s^T = [y_{s1}\,y_{s2}\,y_{s3}] = [x_3\,x_6\,x_9]$ is obtained from the continuous temperature measurements and $y_a^T = [x_1\,x_2\,x_4\,x_5\,x_7\,x_8]$ is obtained from the asynchronously sampled mass fraction measurement. Time varying bounded process noise was added to the simulations.

Table 7. Control parameters for steady states x_{s1} and x_{s2}.

	x_{s1}		x_{s2}
K_1	−5000	K_1	−5000
K_2	−5000	K_2	−5000
K_3	−5000	K_3	−5000
T_i	5 (h)	T_i	5 (h)

Based on the continuous temperature measurements (i.e. y_s), three PI controllers (lower-tier controllers) are first designed following (13) to stabilise system (15) from the initial state $x(0)$ to the steady state x_s using only the heat inputs as the manipulated inputs, which are bounded by $|Q_i| \leq 2 \times 10^6$ KJ/h ($i = 1, 2, 3$). Using the same method as described in Section 4, the parameters of the PI controllers are obtained as shown in Table 7, and two different quadratic Lyapunov functions are obtained, one for each steady state x_{s1}, x_{s2}. The two Lyapunov functions are used to design the upper-tier LMPC controller and the single-tier LMPC controller. The state and input trajectories of system (15) under the lower-tier PI control are shown in Figures 9 and 10. From Figure 9, we see that the PI control law stabilises the temperatures and mass fractions in the three vessels in about 0.7 h for both steady states.

We design next the upper-tier LMPC controller. The feed flow rate to vessel 2, $u_a = F_{20} - F_{20s}$, is the manipulated input for the LMPC, which is bounded by $1 \leq F_{20} \leq 9\,m^3/h$. The performance index is defined by the positive definite function $L(x, u_s, u_a)$ as in (14) in the previous example with Q_c being the following weight matrix:

$$Q_c = \mathrm{diag}\left(\begin{bmatrix} 10^4 & 10^4 & 1 & 10^4 & 10^4 & 1 & 10^4 & 10^4 & 1 \end{bmatrix}\right).$$

diag(V) denotes a matrix with its diagonal elements being the elements of vector V and all the other elements being zeros.

The sampling time of the LMPC is $\Delta = 0.025$ h; the prediction horizon is $\tau_f = 15\Delta$.

Two different simulations have been carried out with different mass fraction measurement sequences $\{t_{k\geq0}\}$ (Figure 11) generated with $W = 1$ and $W = 0.5$ for steady states x_{s1} and x_{s2}, respectively. The average time intervals between two consecutive sampling times are 0.188 h for $W = 1$ and 0.375 h for $W = 0.5$. The state and input trajectories of system (15) under the proposed two-tier control architecture are shown in

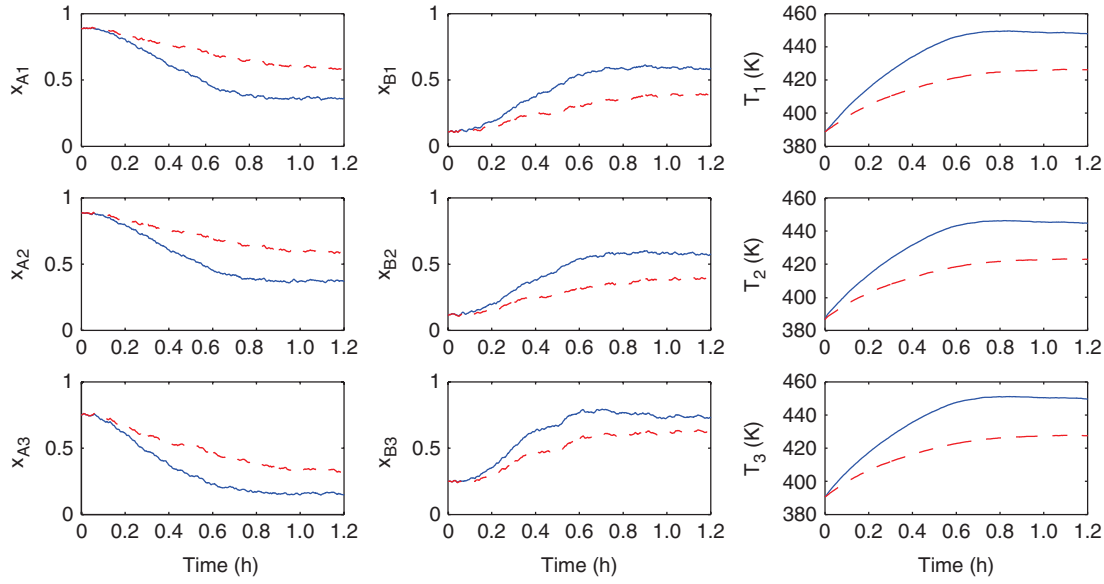

Figure 9. State trajectories of system (15) under lower-tier control law for steady state x_{s1} (solid curves) and steady state x_{s2} (dashed curves).

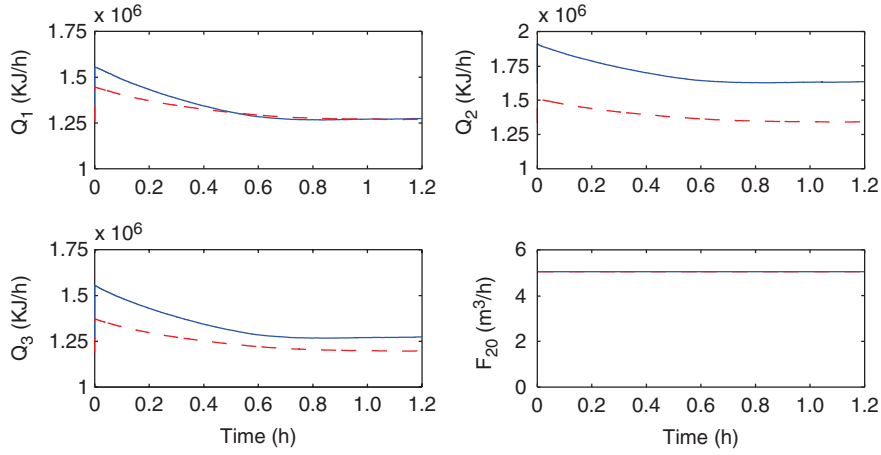

Figure 10. Inputs trajectories of system (15) under lower-tier control law for steady state x_{s1} (solid curves) and steady state x_{s2} (dashed curves).

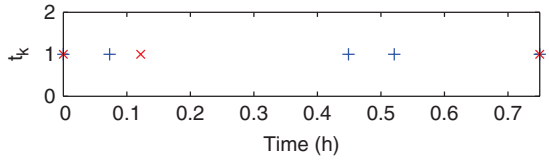

Figure 11. Mass fractions sampling times generated with $W=1$ (+) and $W=0.5$ (×).

Figures 12 and 13. Figure 12 shows that the two-tier control architecture (4) stabilises the temperatures and the mass fractions of the system in about 0.3 h. This implies that the resulting closed-loop system response is faster relative to the speed of the closed-loop response under the low-tier PI controllers.

Another set of simulations was also carried out to compare the proposed two-tier control architecture with the lower-tier controller from a performance index point of view. Table 8 shows the total cost computed for 10 different closed-loop simulations under the proposed two-tier control architecture and the lower-tier controller. To carry out this comparison, we have computed the total cost of each simulation based on the integral of the performance index defined by $L(x, u_s, u_a)$ with different operation conditions in a simulation length of $t_f=0.75$ h. For this set of simulations W is 1. As it can be seen in Table 8, the proposed two-tier control architecture has a cost lower than the corresponding total cost under the lower-tier controller in all the simulations.

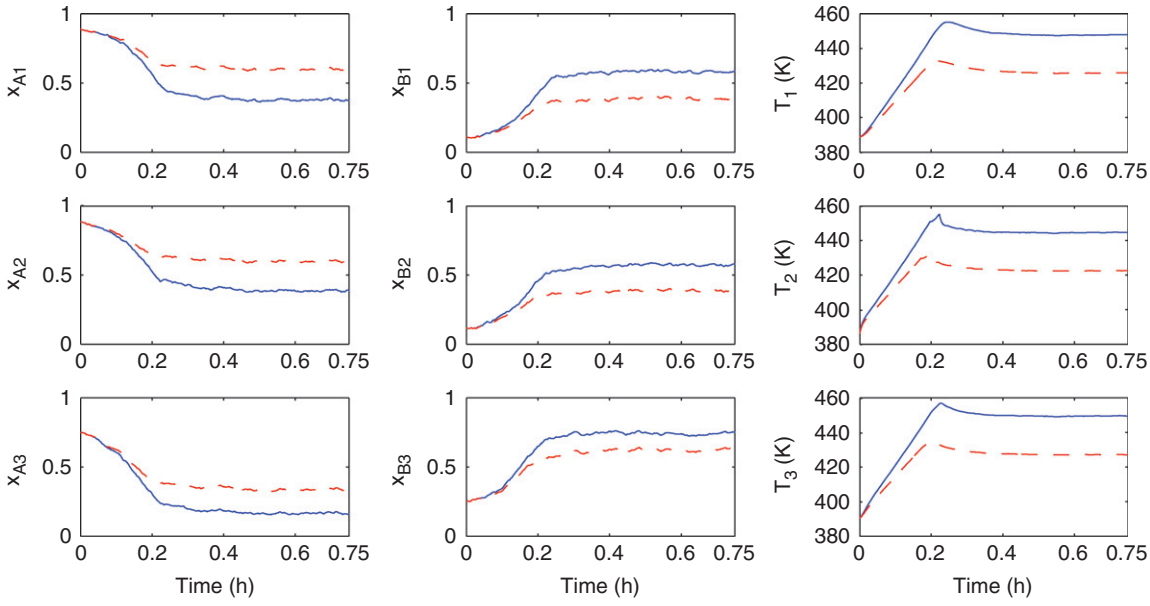

Figure 12. State trajectories of system (15) under the proposed two-tier control architecture when $W = 1$ (solid curves) and $W = 0.5$ (dashed curves).

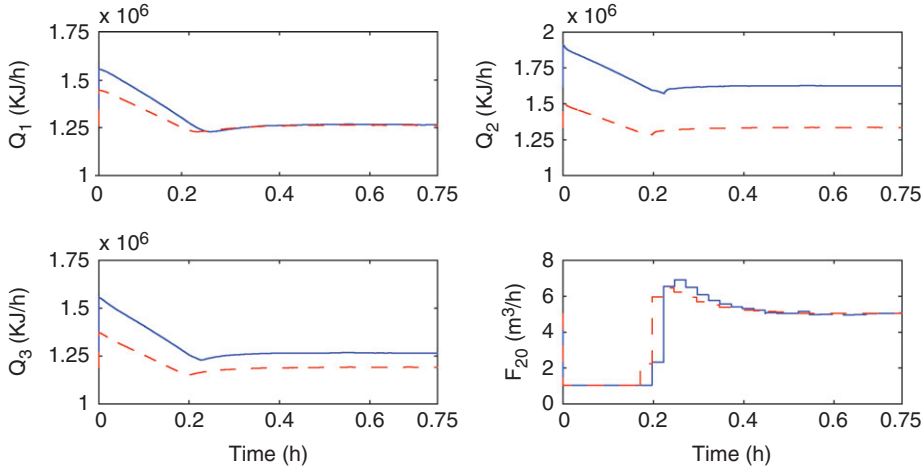

Figure 13. Inputs trajectories of system (15) under the proposed two-tier control architecture when $W = 1$ (solid curves) and $W = 0.5$ (dashed curves).

We have also carried out another set of simulations to compare the computational time needed to evaluate the two-tier LMPC with that of the single-tier LMPC. For these simulations, the single-tier LMPC uses the same parameters as the ones of the two-tier controller in the present example. The simulations have been carried out using Matlab in a Pentium 3.20 GHz. The nonlinear optimisation problem has been solved using the function `fmincom`. To solve the ODEs model (15), both in the simulations and in the optimisation algorithm, an Euler method with a fixed integration time of 0.001 h has been implemented in a mex DLL

Table 8. Total performance cost along the closed-loop trajectories.

Sim.	Two-tier	PI controllers	Sim.	Two-tier	PI controllers
1	1.179×10^5	2.760×10^5	6	1.560×10^5	3.742×10^5
2	1.164×10^5	2.795×10^5	7	1.645×10^5	3.951×10^5
3	1.273×10^5	2.991×10^5	8	1.701×10^5	4.107×10^5
4	1.351×10^5	3.177×10^5	9	1.962×10^5	4.408×10^5
5	1.364×10^5	3.240×10^5	10	1.848×10^5	4.492×10^5

using the C Programming Language. The mean time to solve the LMPC optimisation problem of this set of simulations is 23.24 s for the two-tier LMPC and 37.59 s for the single-tier LMPC. From this set of simulations, we see that the computation time needed to solve the single-tier LMPC optimisation problem is substantially larger even though the closed-loop performance in terms of the total performance cost is comparable to the one of the two-tier control architecture. This is because the single-tier LMPC has to optimise both the inputs u_s and u_a.

6. Conclusion

In this work, a two-tier control architecture was proposed for nonlinear process systems with both continuous and asynchronous measurements. The two-tier control architecture takes advantage of both the continuous and asynchronous measurements to improve the performance of the closed-loop system while guaranteeing that the stability properties obtained by the lower tier controller are maintained. While classical control schemes can be used at the lower tier, a LMPC scheme was proposed as the upper-tier controller to explicitly account for asynchronous measurements and the influence of the lower-tier controller on the closed-loop system. The proposed two-tier control architecture was demonstrated through two chemical process examples.

Acknowledgement

Financial support from NSF and European Commission, INFSOICT-223866, is gratefully acknowledged.

References

Brockett, R.W., and Liberzon, D. (2000), 'Quantized Feedback Stabilization of Linear Systems', *IEEE Transactions on Automatic Control*, 45, 1279–1289.

Christofides, P.D., Davis, J.F., El-Farra, N.H., Clark, D., Harris, K.R.D., and Gipson, J.N. (2007), 'Smart Plant Operations: Vision, Progress and Challenges', *AIChE Journal*, 53, 2734–2741.

Christofides, P.D., and El-Farra, N.H. (2005), *Control of Nonlinear and Hybrid Process Systems: Designs for Uncertainty, Constraints And Time-delays*, Berlin, German: Springer-Verlag.

Davis, J.F. (2007), 'Report from NSF Workshop on Cyberinfrastructure in Chemical and Biological Systems: Impact and Directions', Technical Report, http://www.oit.ucla.edu/nsfci/NSFCIFullReport.pdf for the pdf file of this report.

Hassibi, A., Boyd, S.P., and How, J.P. (1999), 'Control of Asynchronous Dynamical Systems with Rate Constraints on Events', in *Proceedings of Conference on Decision and Control*, pp. 1345–1351.

Hespanha, J.P. (2005), 'A Model for Stochastic Hybrid Systems with Application to Communication Networks', *Nonlinear Analysis – Theory Methods and Applications*, 62, 1353–1383.

Hong, S.H. (1995), 'Scheduling Algorithm of Data Sampling Times in the Integrated Communication and Control-systems', *IEEE Transactions On Control Systems Technology*, 3, 225–230.

Khalil, H.K. (1996), *Nonlinear Systems* (2nd ed.), Englewood Cliffs, NJ: Prentice Hall.

Mao, X. (1999), 'Stability of Stochastic Differential Equations with Markovian Switching', *Stochastic Processes and their Applications*, 79, 45–67.

Mayne, D.Q., Rawlings, J.B., Rao, C.V., and Scokaert, P.O.M. (2000), 'Constrained Model Predictive Control: Stability and Optimality', *Automatica*, 36, 789–814.

Mhaskar, P., Gani, A., McFall, C., Christofides, P.D., and Davis, J.F. (2007), 'Fault-tolerant Control of Nonlinear Process Systems Subject to Sensor Faults', *AIChE Journal*, 53, 654–668.

Mhaskar, P., El-Farra, N.H., and Christofides, P.D. (2005), 'Predictive Control of Switched Nonlinear Systems with Scheduled Mode Transitions', *IEEE Transactions on Automatic Control*, 50, 1670–1680.

Mhaskar, P., El-Farra, N.H., and Christofides, P.D. (2006), 'Stabilization of Nonlinear Systems with State and Control Constraints using Lyapunov-based Predictive Control', *Systems and Control Letters*, 55, 650–659.

Muñoz de la Peña, D., and Christofides, P.D. (2008a), 'Lyapunov-based Model Predictive Control of Nonlinear Systems Subject to Data Losses', *IEEE Transactions on Automatic Control*, 53, 2076–2089.

Muñoz de la Peña, D., and Christofides, P.D. (2008b), 'Stability of Nonlinear Asynchronous Systems', *Systems and Control Letters*, 57, 465–473.

Nair, G.N., and Evans, R.J. (2000), 'Stabilization with Data-rate-limited Feedback: Tightest Attainable Bounds', *Systems and Control Letters*, 41, 49–56.

Nešić, D., and Teel, A.R. (2004), 'Input – Output Stability Properties of Networked Control Systems', *IEEE Transactions on Automatic Control*, 49, 1650–1667.

Nešić, D., Teel, A., and Kokotovic, P. (1999), 'Sufficient Conditions for Stabilization of Sampled-data Nonlinear Systems via Discrete Time Approximations', *Systems and Control Letters*, 38, 259–270.

Neumann, P. (2007), 'Communication in Industrial Automation: What is Going on?', *Control Engineering Practice*, 15, 1332–1347.

Nguyen, G.T., Katz, R.H., Noble, B., and Satyanarayananm, M. (1996), 'A Tracebased Approach for Modeling Wireless Channel Behaviour', in *Proceedings of Winter Simulation Conference*, pp. 597–604.

Ploplys, N.J., Kawka, P.A., and Alleyne, A.G. (2004), 'Closed-loop Control Over Wireless Networks – Developing a Novel Timing Scheme for Real-time Control Systems', *IEEE Control Systems Magazine*, 24, 52–71.

Rawlings, J.B. (2000), 'Tutorial Overview of Model Predictive Control', *IEEE Control Systems Magazine*, 22, 38–52.

Ritchey, V.S., and Franklin, G.F. (1989), 'A Stability Criterion for Asynchronous Multirate Linear Systems', *IEEE Transactions on Automatic Control*, 34, 529–535.

Shin, K.G. (1991), 'Real-time Communications in a Computer-controlled Workcell', *IEEE Transactions on Robotics and Automation*, 7, 105–113.

Su, Y.F., Bhaya, A., Kaszkurewicz, E., and Kozyakin, V.S. (1997), 'Further Results on Stability of Asynchronous Discrete-time Linear Systems', in *Proceedings of Conference on Decision and Control*, San Diego, CA, pp. 915–920.

Tabbara, M., Nešić, D., and Teel, A.R. (2007), 'Stability of Wireless and Wireline Networked Control Systems', *IEEE Transactions on Automatic Control*, 52, 1615–1630.

Tabuada, P., and Wang, X. (2006), 'Preliminary Results on State-triggered Scheduling of Stabilizing Control Tasks', in *Proceedings of Conference on Decision and Control*, pp. 282–287.

Walsh, G., Ye, H., and Bushnell, L. (2002), 'Stability Analysis of Networked Control Systems', *IEEE Transactions on Control Systems Technology*, 10, 438–446.

Ydstie, E.B. (2002), 'New Vistas for Process Control: Integrating Physics and Communication Networks', *AIChE Journal*, 48, 422–426.

Ye, H., and Walsh, G. (2001), 'Real-time Mixed-traffic Wireless Networks', *IEEE Transactions on Industrial Electronics*, 48, 883–890.

Ye, H., Walsh, G., and Bushnell, L. (2000), 'Wireless Local Area Networks in the Manufacturing Industry', in *Proceedings of American Control Conference*, pp. 2363–2367.